Electronic Supplementary Material (ESI) for ChemComm.
This journal is © The Royal Society of Chemistry 2023

Supporting Information

A Photoresponsive Gold Catalyst Based on Azobenzene-Functionalized NHC Ligands

Jianghua Liu, Eduard O. Bobylev, Bas de Bruin and Joost N. H. Reek*

Contents

1. Materials and devices 1

2. Synthesis and characterization of catalyst Azo-NHC-Au 1

3. Photoswitchable properties of ligand Azo-NHC 5

4. Photoswitchable properties of catalyst Azo-NHC-Au 7

5. Stability of *cis*-Cat 8

6. Catalysis 9

7. Computational study (DFT) for *trans*-Cat, *cis*-Cat structure optimization 14

8. Steric maps and buried volume of *trans*-Cat and *cis*-Cat 15

9. References 15

10. Cartesian coordinates of optimized configurations of *trans*-Cat and *cis*-Cat 16

1. Materials and devices

All reagents and solvents were commercially available and used without further purification, unless otherwise noted. NMR spectrum (^{1}H, ^{13}C) were measured on Bruker AV400 MHz instrument, and chemical shifts were recorded in parts per million (ppm) using deuterated solvent residual signal as reference. High resolution mass (HRMS) spectrum were collected on an AccuTOF-LC, JMS-T100LP Mass spectrometer (JEOL, Japan) (for ESI) and an AccuTOF-GC v 4g, JMS-T100GCV Mass spectrometer (JEOL, Japan) (for FD). UV-vis spectrum were performed on a single beam Hewlett Packard 8453 spectrometer in a quartz cuvette (light path 10 mm) at 25 °C with a PTC-348WI temperature controller using THF:H_2O = 1:1 as background. 365 nm light source: BAI BLB Fluorescent Tube T5 G5 4W 08 Blacklight Blue 16 x 136 mm UV lamp. 470 nm light source: LED lighting modules 20Pcs DC 12V 3 SMD-5630-LEDs module waterproof super bright blue light.

2. Synthesis and characterization of catalyst Azo-NHC-Au

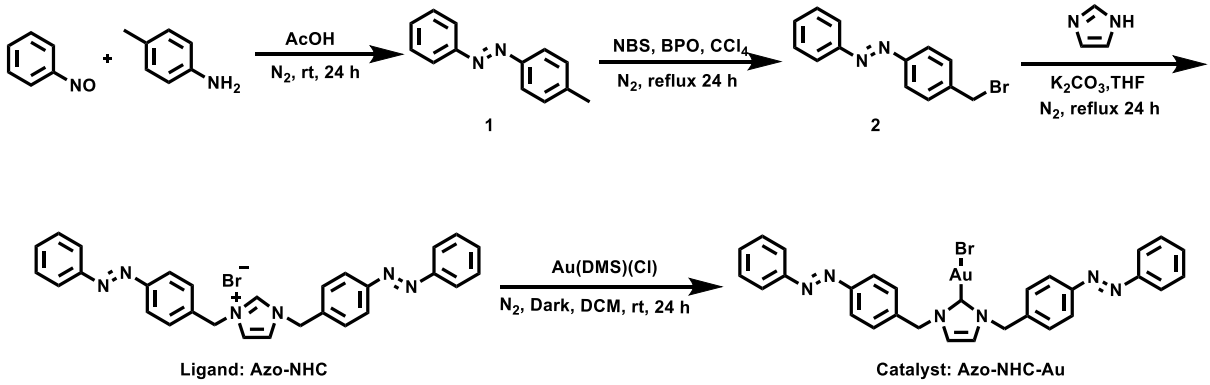

Scheme S1. Synthesis of ligand Azo-NHC and catalyst Azo-NHC-Au.

(*E*)-1-phenyl-2-(*p*-tolyl)diazene (1):

1 was prepared according to the previous literature.[1–5]

(*E*)-1-(4-(bromomethyl)phenyl)-2-phenyldiazene (2):

2 was prepared according to the previous literature.[1–5]

1,3-bis(4-((*E*)-phenyldiazenyl)benzyl)-1*H*-imidazol-3-ium bromide (Ligand: Azo-NHC):

A mixture of **2** (515.15 mg, 1.88 mmol), imidazole (58.75 mg, 0.86 mmol) and K_2CO_3 (360 mg, 2.60 mmol) in dry THF (10 mL) were refluxed for 24 h under N_2. After cooling down to room temperature, the mixture was concentrated. Water was added and extracted with dichloromethane. The combined organic phases were dried over $MgSO_4$ and filtrate was evaporated under reduced pressure. The residue was purified by column chromatographically on silica gel (MeOH/CH_2Cl_2, 5:95) to afford **Azo-NHC** as an orange solid (283.9 mg, 61%). ^{1}H NMR (400 MHz, $CDCl_3$) δ (ppm): 10.93 (s, 1H), 7.97 (d, *J* = 8.0 Hz, 4H), 7.92 (d, *J* = 8.0 Hz, 4H), 7.61 (d, *J* = 8.1 Hz, 4H), 7.52 (m, 6H), 7.11 (s, 2H), 5.67 (s, 4H); ^{13}C NMR (101 MHz, $CDCl_3$) δ

(ppm): 153.4, 152.6, 138.6, 134.8, 131.8, 130.1, 129.3, 124.1, 123.2, 121.7, 53.7. HRMS (ESI): calc. for $[M\text{-}Br]^+$ ($C_{29}H_{25}N_6^+$) m/z 457.2141, found 457.2638.

(1,3-bis(4-((*E*)-phenyldiazenyl)benzyl)-2,3-dihydro-1*H*-imidazol-2-yl)gold(II) bromide (Catalyst: Azo-NHC-Au):

A mixture of **Azo-NHC** (26.81 mg, 0.05 mmol), Chloro(dimethylsulfide)gold(I) (14.73 mg, 0.05 mmol) and K_2CO_3 (6.91 mg, 0.05 mmol) in acetone (2 mL) were refluxed at room temperature for 24 h. After cooling down to room temperature, the solvents were removed under reduced pressure, and 5 mL dichloromethane was added and filtered through a pad of celite. The filtrate was concentrated under reduced pressure and 10 mL pentane was added to obtain orange precipitate. The crude product was centrifuged and washed with pentane (3×5 mL), and dried under vacuum to afford **Azo-NHC-Au** as an orange solid (26.76 mg, 73%). ^{1}H NMR (400 MHz, $CDCl_3$) δ (ppm): 7.92 (m, 8H), 7.51 (m, 10H), 6.93 (s, 2H), 5.51 (s, 4H). ^{13}C NMR (101 MHz, $CDCl_3$) δ (ppm): 175.4, 152.8, 152.5, 137.3, 131.4, 129.2, 128.9, 123.6, 123.0, 121.0, 54.9. HRMS (FD): calc. for [M] ($C_{29}H_{24}N_6Au_1Br_1$) 734.0895, found 734.0872.

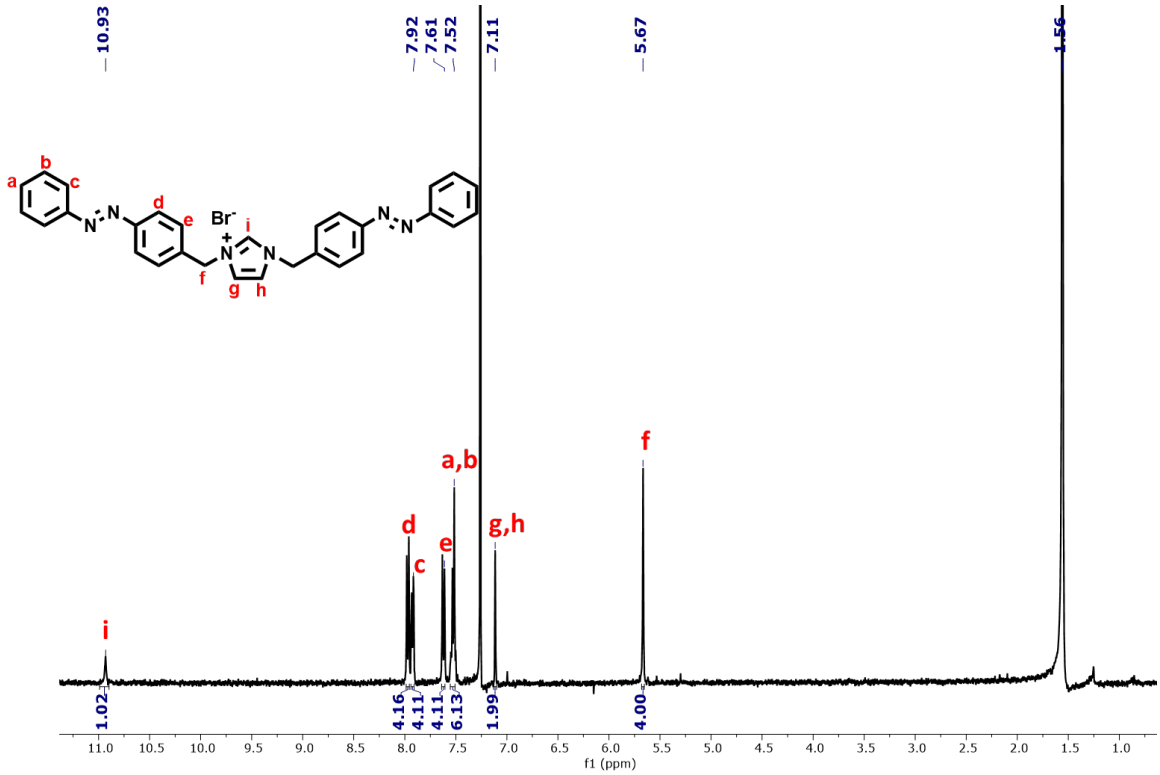

Figure S1. ^{1}H NMR spectrum (400 MHz, 298 K) of ligand Azo-NHC in $CDCl_3$.

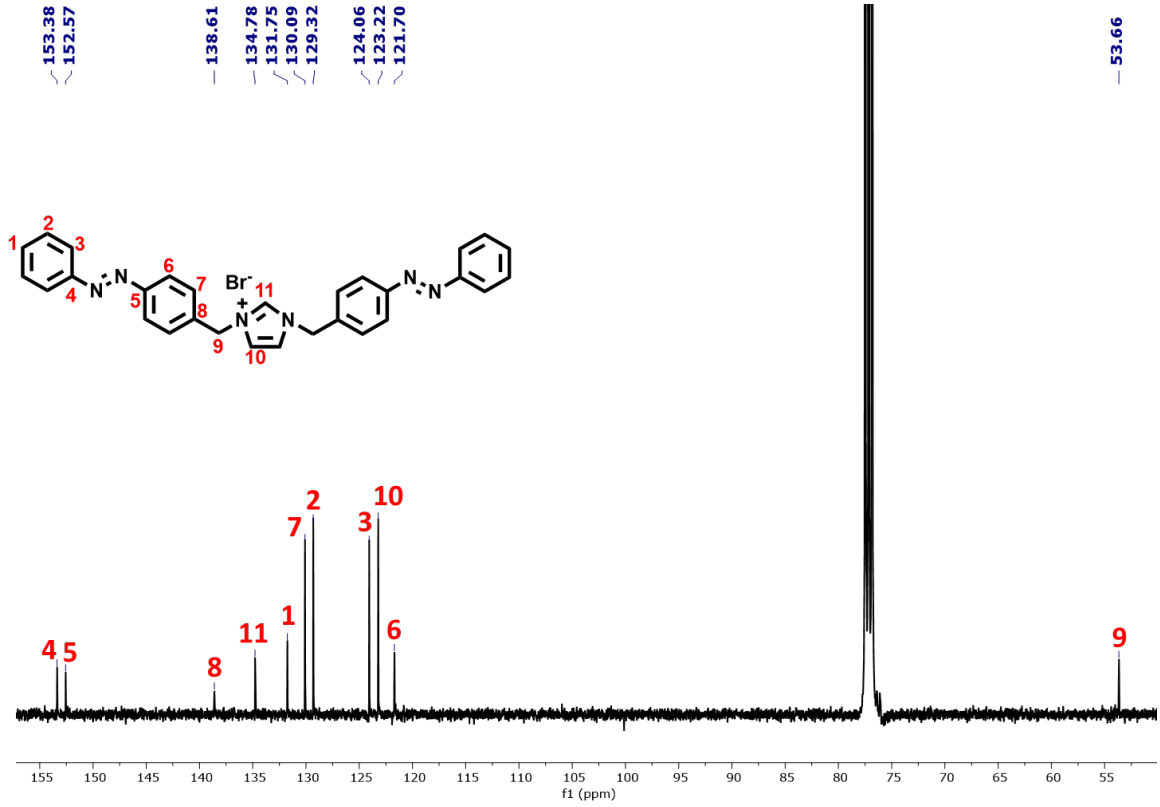

Figure S2. ^{13}C NMR spectrum (101 MHz, 298 K) of ligand Azo-NHC in $CDCl_3$.

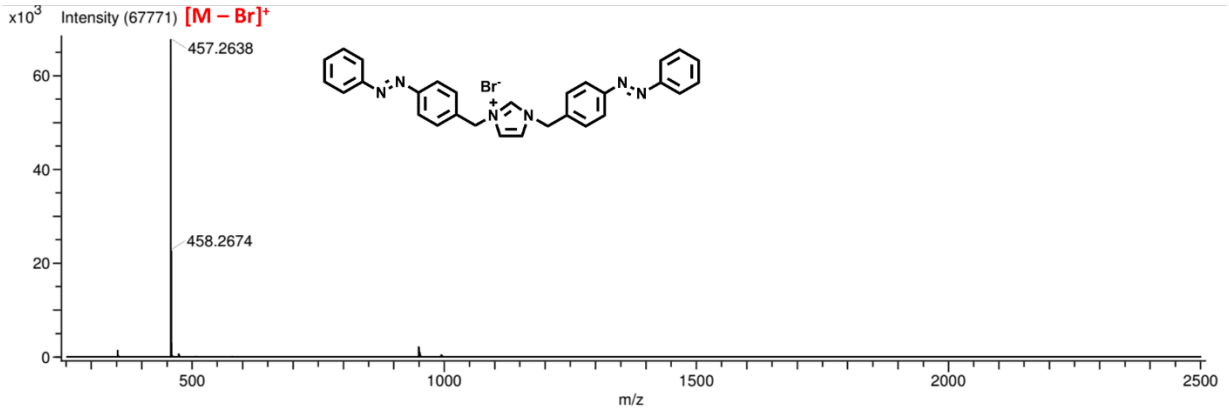

Figure S3 . ESI-Mass spectrum of ligand Azo-NHC.

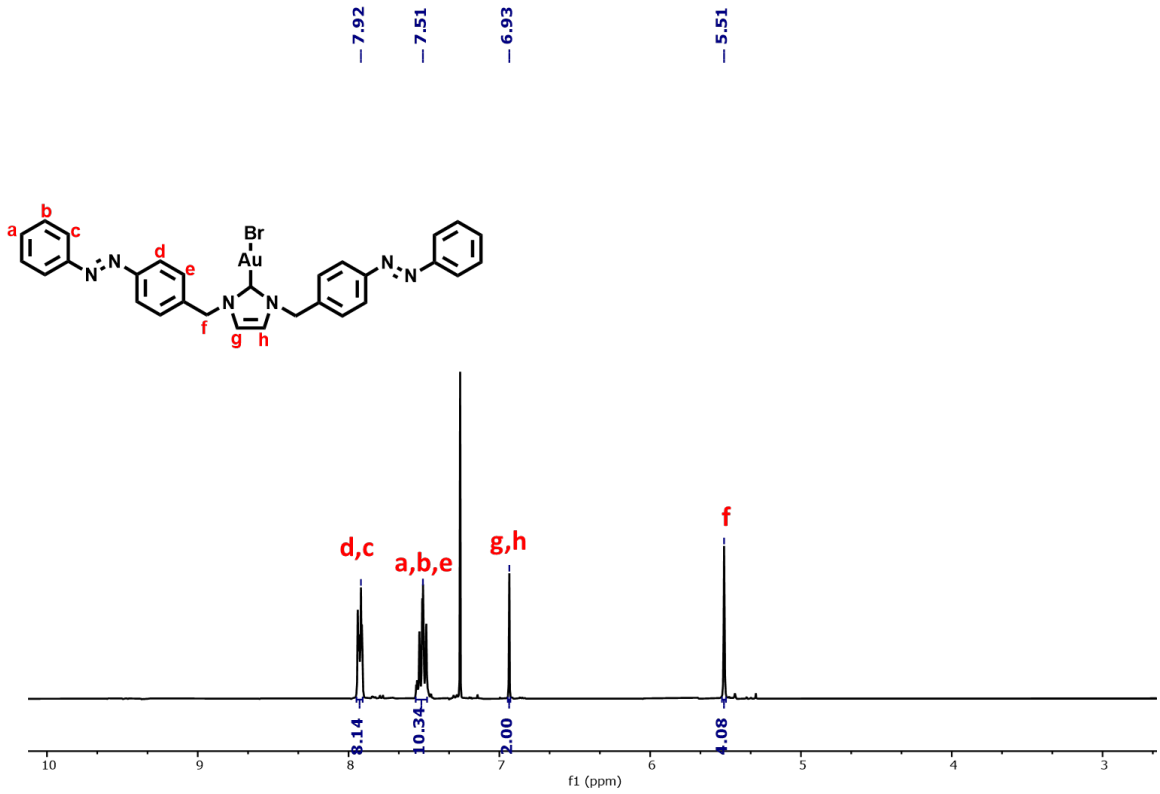

Figure S4 . ^{1}H NMR spectrum (400 MHz, 298 K) of catalyst Azo-NHC-Au in $CDCl_3$.

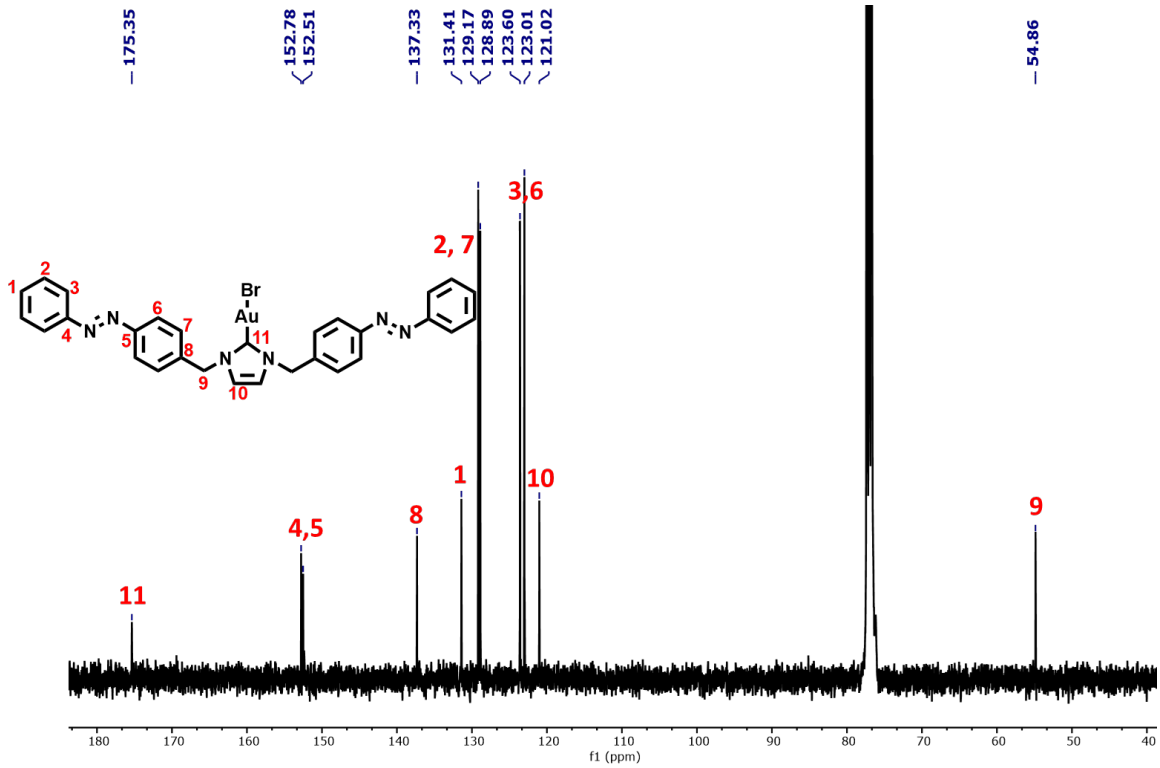

Figure S5 . ^{13}C NMR spectrum (101 MHz, 298 K) of catalyst Azo-NHC-Au in $CDCl_3$.

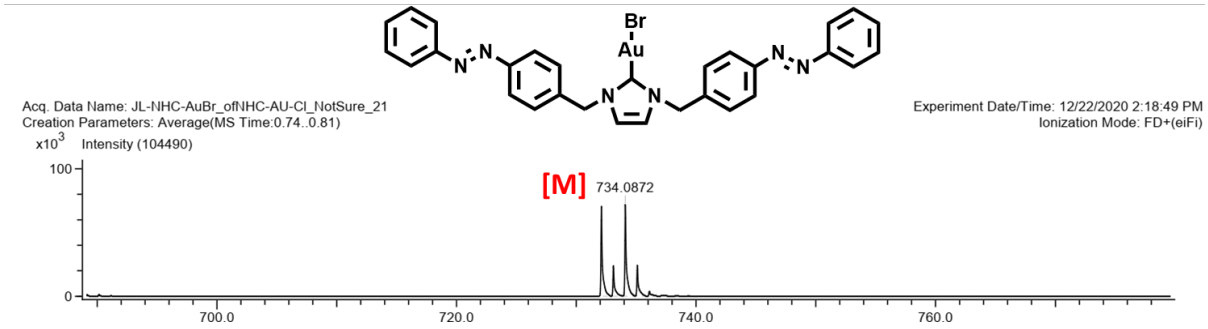

Figure S6 . FD-Mass spectrum of catalyst Azo-NHC-Au.

3. Photoswitchable properties of ligand Azo-NHC

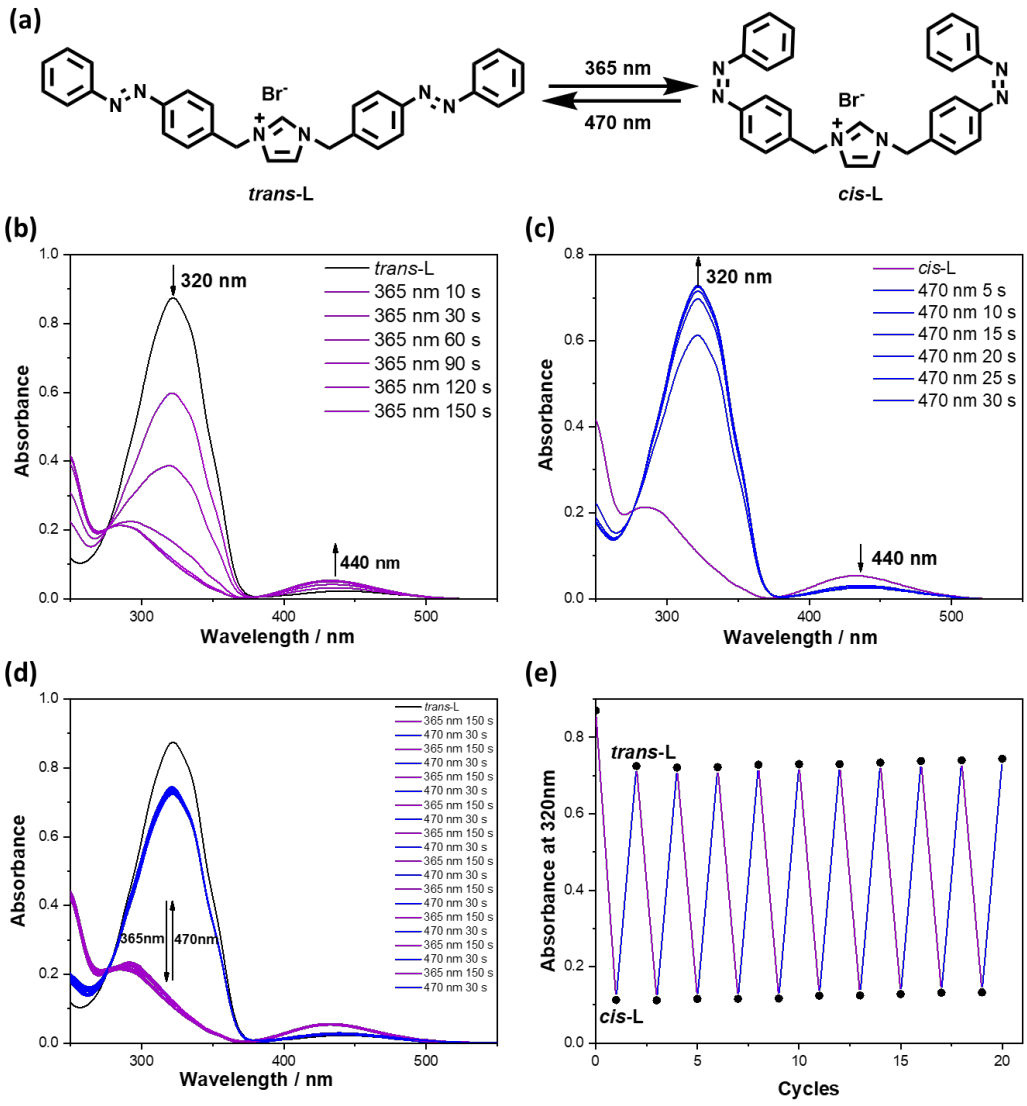

Figure S7. (a) Photoswitching between *trans*-L and *cis*-L; (b) Absorption changes after irradiating *trans*-L by 365 nm light for different time until reaching photostationary state; (c) Absorption changes after irradiating *cis*-L by 470 nm light for different time until reaching another photostationary state; (d) Reversible transform between *trans*-L and *cis*-L; (e)

Recyclability between *trans*-L and *cis*-L recording the absorption at 320 nm. ([*trans*-L] = 20 uM in THF:H_2O = 1:1 at 298 K).

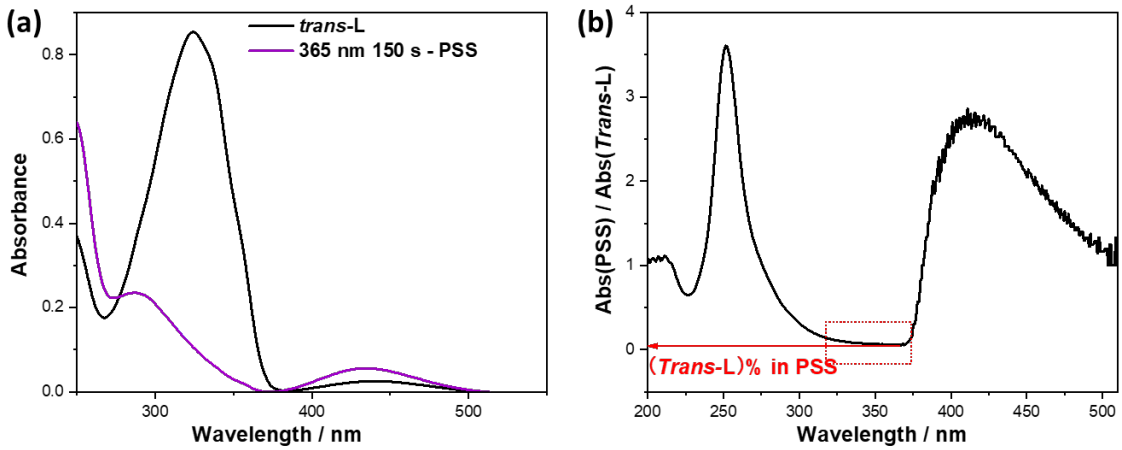

Figure S8. (a) Absorption of *trans*-L and photostationary state (PSS) obtained from irradiating *trans*-L by 365 nm light for 150 s; (b) Abs(PSS)/Abs(*trans*-L) ratio versus wavelength: the curve in red box remains horizontal denotes that only the *trans*-L absorbs but not the *cis*-L Thus, this ratio Abs(PSS)/Abs(*trans*-L) represents the *trans*-L content in PSS. In this case, PSS = 5% *trans*-L + 95% *cis*-L.

4. Photoswitchable properties of catalyst Azo-NHC-Au

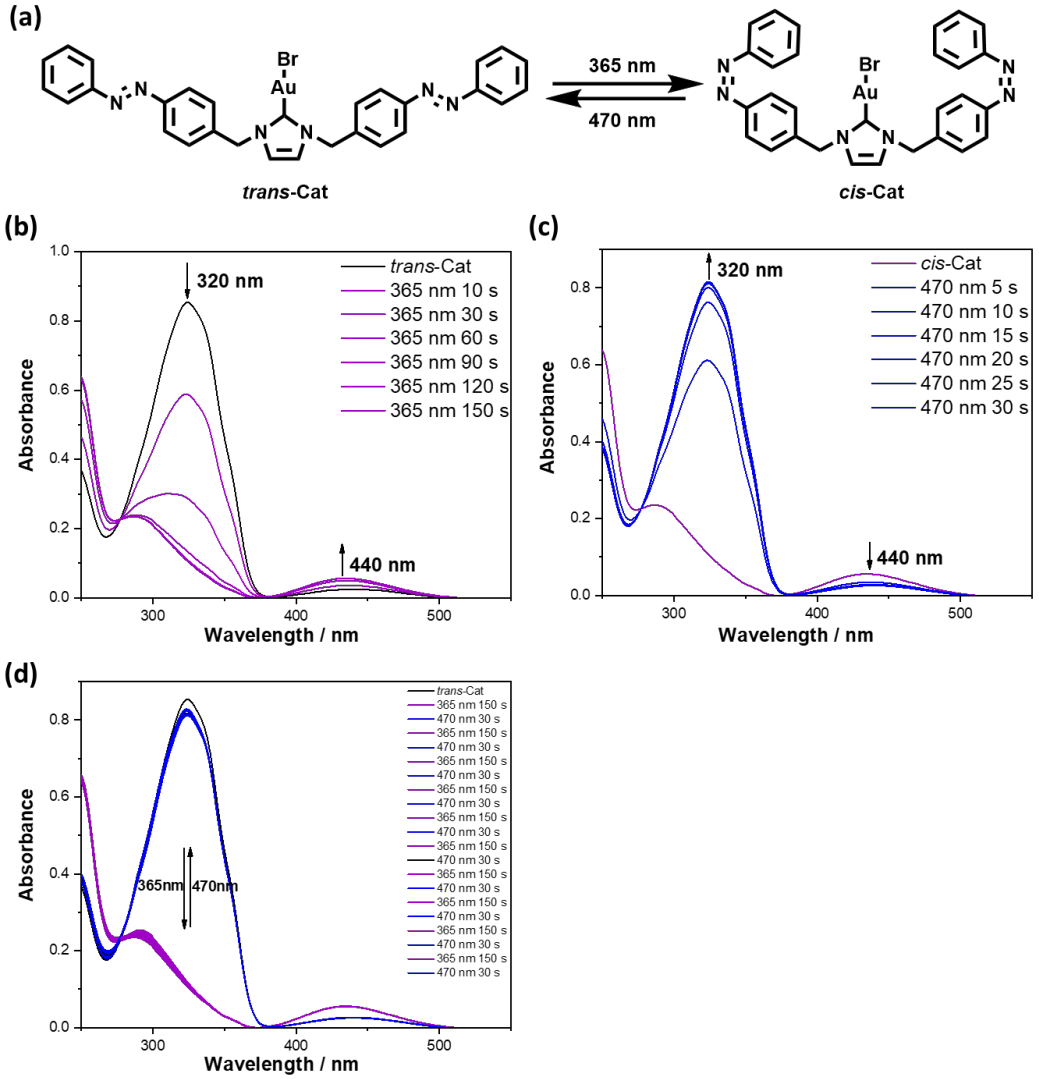

Figure S9. (a) Photoswitching between *trans*-Cat and *cis*-Cat; (b) Absorption changes after irradiating *trans*-Cat by 365 nm light for different time until reaching photostationary state; (c) Absorption changes after irradiating *cis*-Cat by 470 nm light for different time until reaching another photostationary state; (d) Reversible transform between *trans*-Cat and *cis*-Cat. ([*trans*-Cat] = 20 uM in THF:H_2O = 1:1 at 298 K).

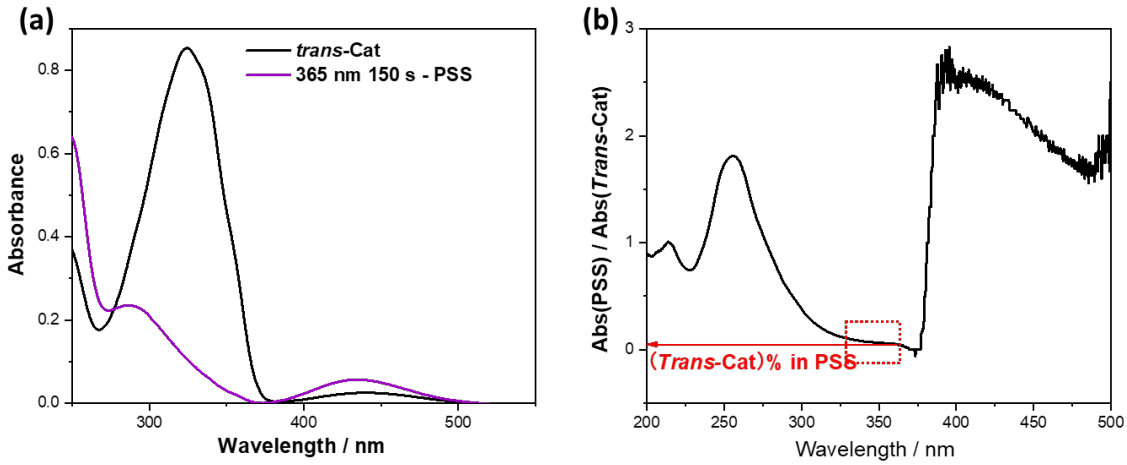

Figure S10. (a) Absorption of *trans*-Cat and photostationary state (PSS) obtained from irradiating *trans*-Cat by 365 nm light for 150 s; (b) Abs(PSS)/Abs(*trans*-Cat) ratio versus wavelength: the curve in red box remains horizontal denotes that only the *trans*-Cat absorbs but not the *cis*-Cat. Thus, this ratio Abs(PSS)/Abs(*trans*-Cat) represents the *trans*-Cat content in PSS. In this case, PSS = 5% *trans*-Cat + 95% *cis*-Cat.

5. Stability of *cis*-Cat

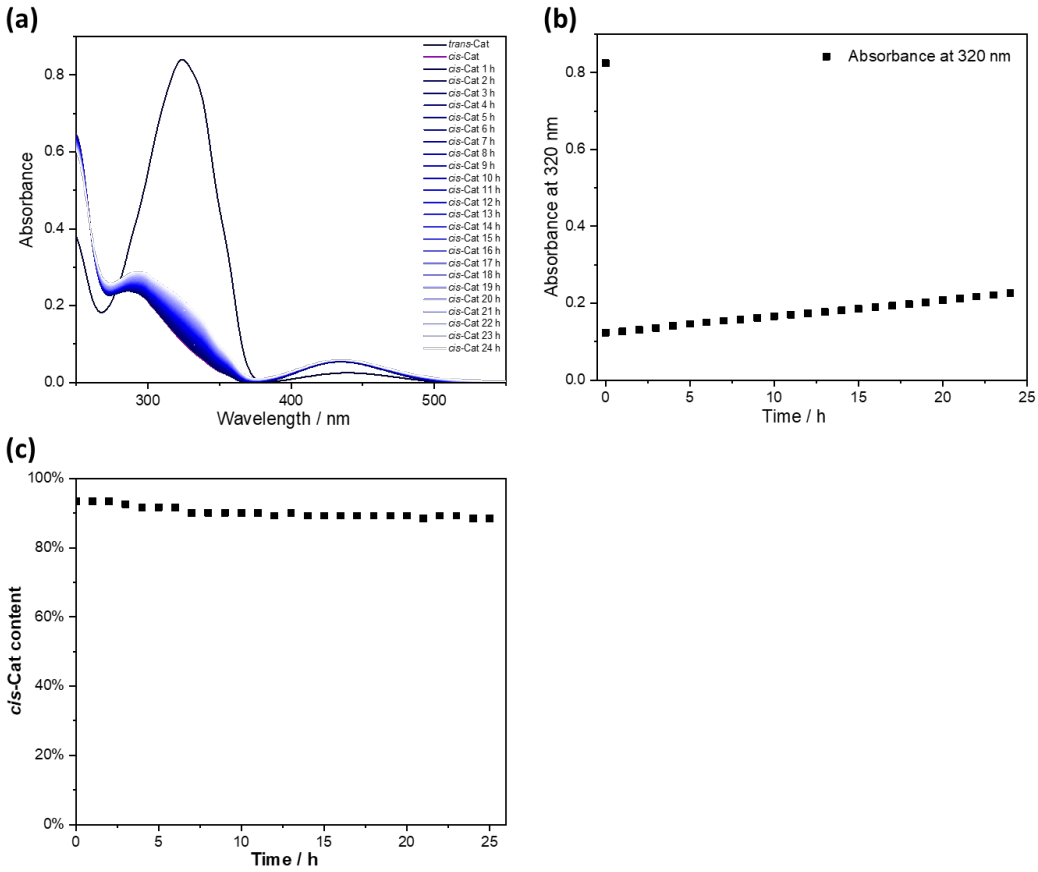

Figure S11. (a) UV-vis absorption spectrum recording the thermal relaxation of *cis*-Cat in dark every 1 h within 24 h; (b) Stability of *cis*-Cat recorded by the absorption changed at 320 nm; (c) Thermal stability of *cis*-Cat within 24 h at dark monitored every 1 h by ^{1}H NMR (Concentration of UV-vis: [*trans*-Cat] = 20 uM in THF:H_2O = 1:1 at 298 K, ^{1}H NMR: [*trans*-Cat] = 500 uM in THF-d_8:D_2O = 1:1 at 298 K).

6. Catalysis

All the reactions were carried out in THF-d_8:D_2O = 1:1 at room temperature. Reagent concentrations for stock solution: [substrate 3] = 10 mM in THF-d_8, [*trans*-Cat] = 1 mM in THF-d_8, [Internal standard] = 6.67 mM in THF-d_8. For *trans*-Cat catalytic reaction: in a 2 mL glass vial covered by aluminum foil, 60 uL substrate, 60 uL internal standard, 120 uL THF-d_8, 300 uL D_2O, 60 uL *trans*-Cat were mixed together and then the reaction kinetics were monitored every 1 h automatically by ^{1}H NMR in 24 h. For *cis*-Cat catalytic reaction: in a 2 mL glass vial covered by aluminum foil, 60 uL *trans*-Cat, 120 uL THF-d_8, 300 uL D_2O were mixed together and irradiated by 365 nm light for 10 min to get the *cis*-Cat. And then 60 uL internal standard and 60uL substrate were added and then the reaction kinetics were monitored every 1 h automatically in 24 h. The final concentration for reaction solution are: [substrate] = 1 mM, [Cat] = 0.1 mM (10%), [Internal standard] = 0.67 mM in THF-d_8:D_2O = 1:1. The NHC-Au-Br catalyst was activated in situ by D_2O. The conversion and yield were calculated based on ^{1}H NMR integration by using 1,3,5-trimethoxybenzene as an internal standard (error 5%).

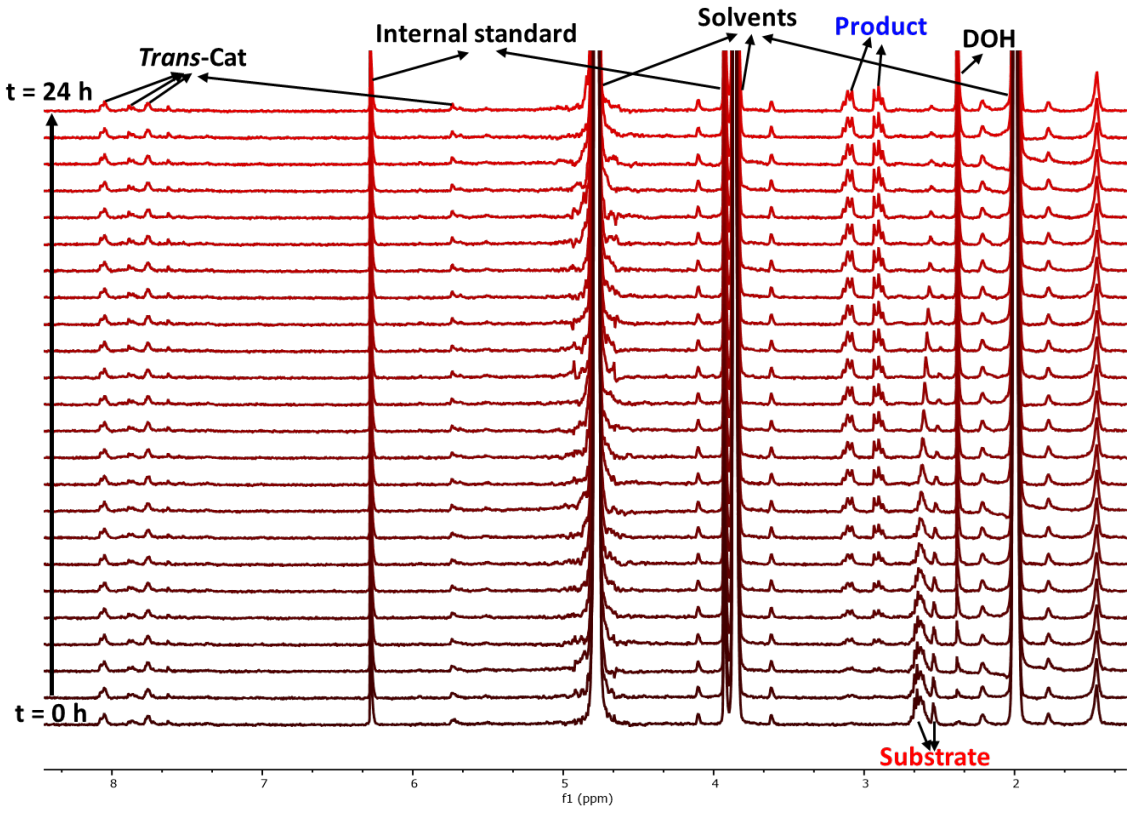

Figure S12. ^{1}H NMR (300 MHz, 298 K) monitored the catalytic reaction process by *trans*-Cat every 1 h in THF-d_8:D_2O = 1:1 for 24 h. All the signals for the substrate 3, product 4, *trans*-Cat, solvents and internal standard can be clearly assigned.

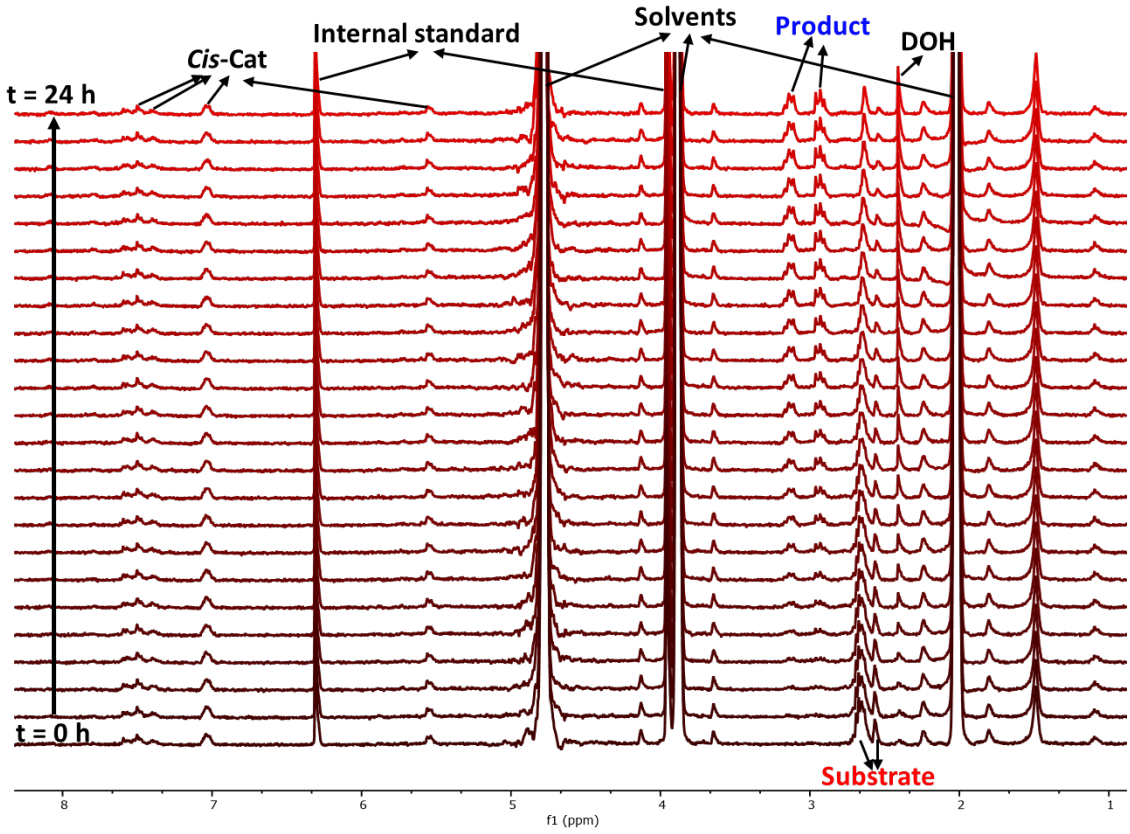

Figure S13. ^{1}H NMR (300 MHz, 298 K) monitored the catalytic reaction process by *cis*-Cat every 1 h in THF-d_8:D_2O = 1:1 for 24 h. All the signals for the substrate 3, product 4, *cis*-Cat, solvents and internal standard can be clearly assigned.

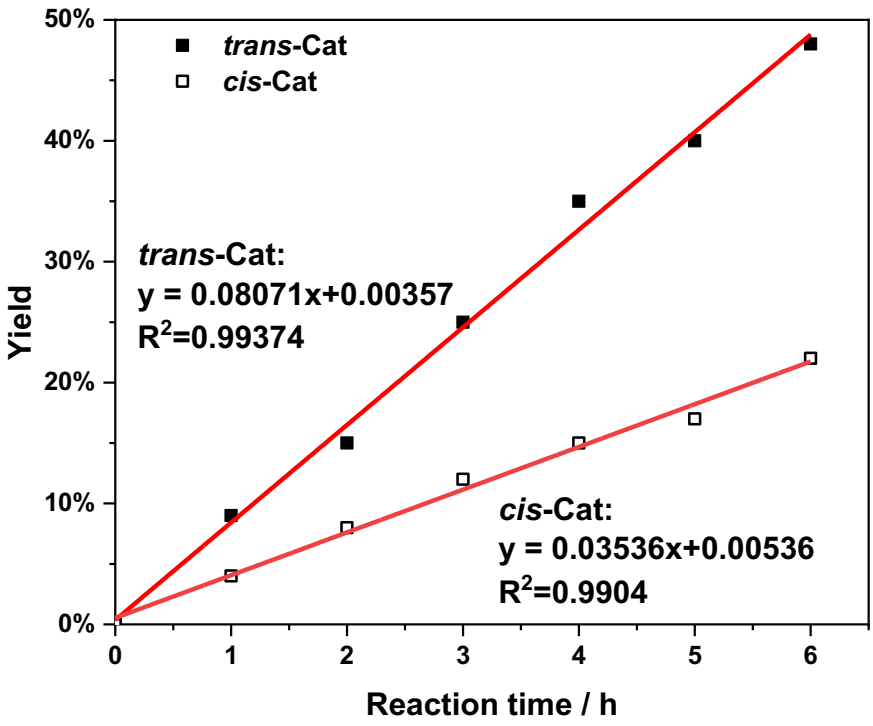

Figure S14. Reaction rate based on the linear fit of product 4 yield in 6 h (figure 3b).

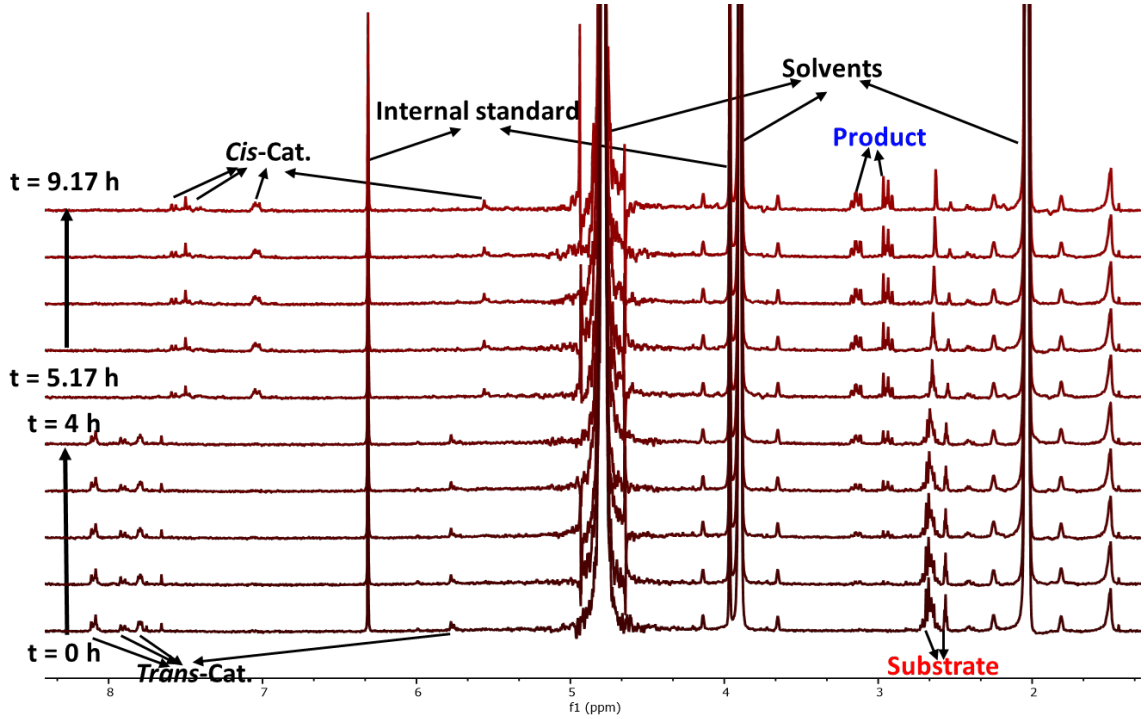

Figure S15. ^{1}H NMR (300 MHz, 298 K) monitored the catalytic reaction process every 1 h in THF-d_8:D_2O = 1:1 for 9 h. In first four hours, reaction was catalyzed by *trans*-Cat and then after 10 min 365 nm irradiation to generate *cis*-Cat in situ for the next four hours' catalysis. All the signals for the substrate 3, product 4, *trans*-Cat, *cis*-Cat, solvents and internal standard can be clearly assigned.

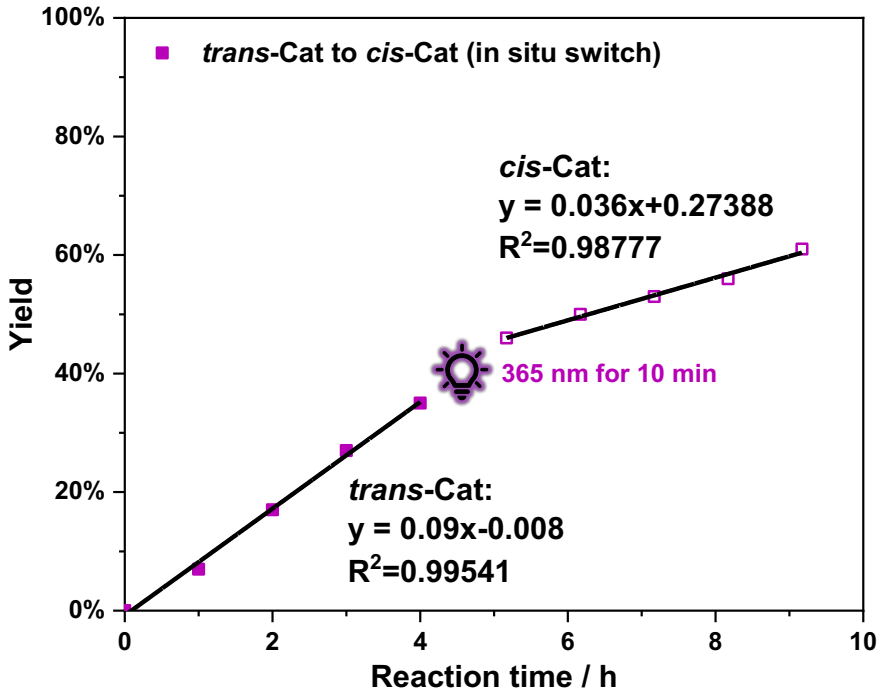

Figure S16. Reaction rate based on the linear fit of product 4 yield, *trans*-Cat for 0-4 h, *cis*-Cat for 5-9 h (Figure 3c purple).

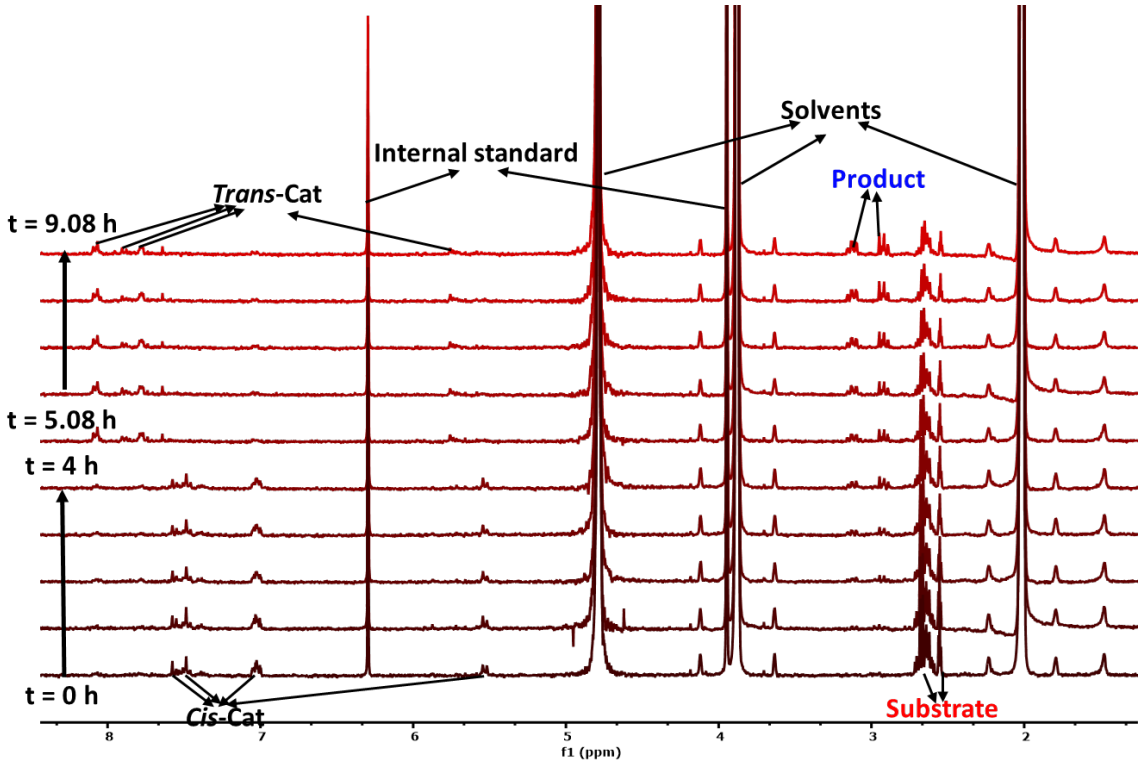

Figure S17. ^{1}H NMR (300 MHz, 298 K) monitored the catalytic reaction process every 1 h in THF-d_8:D_2O = 1:1 for 9 h. In first four hours, reaction was catalyzed by *cis*-Cat and then after

5 min 470 nm irradiation to generate *trans*-Cat in situ for the next four hours' catalysis. All the signals for the substrate 3, product 4, *trans*-Cat, *cis*-Cat, solvents and internal standard can be clearly assigned.

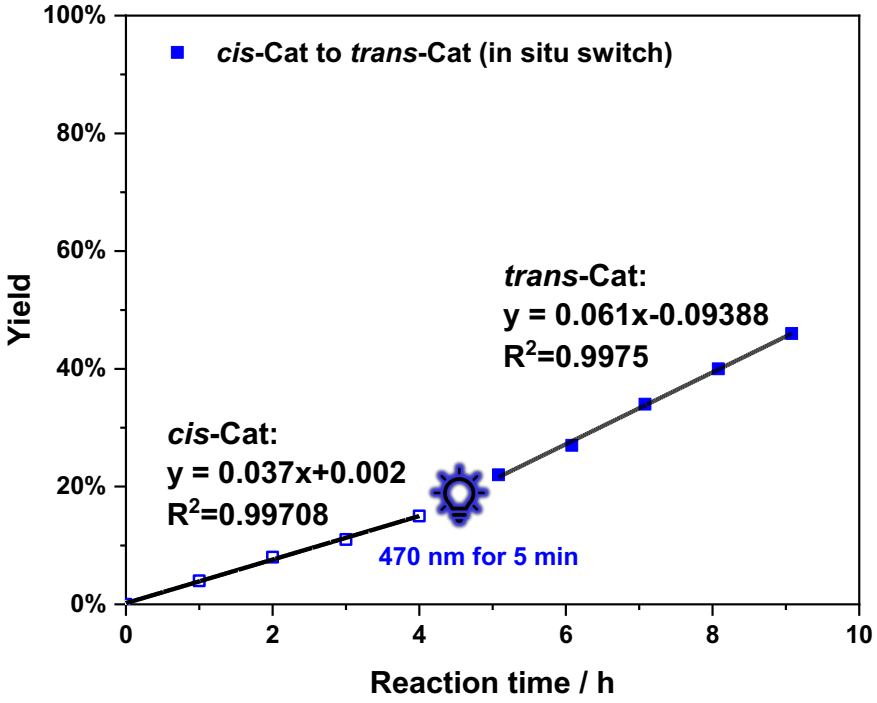

Figure S18. Reaction rate based on the linear fit of product 4 yield, *cis*-Cat for 0-4 h, *trans*-Cat for 5-9 h (Figure 3c blue).

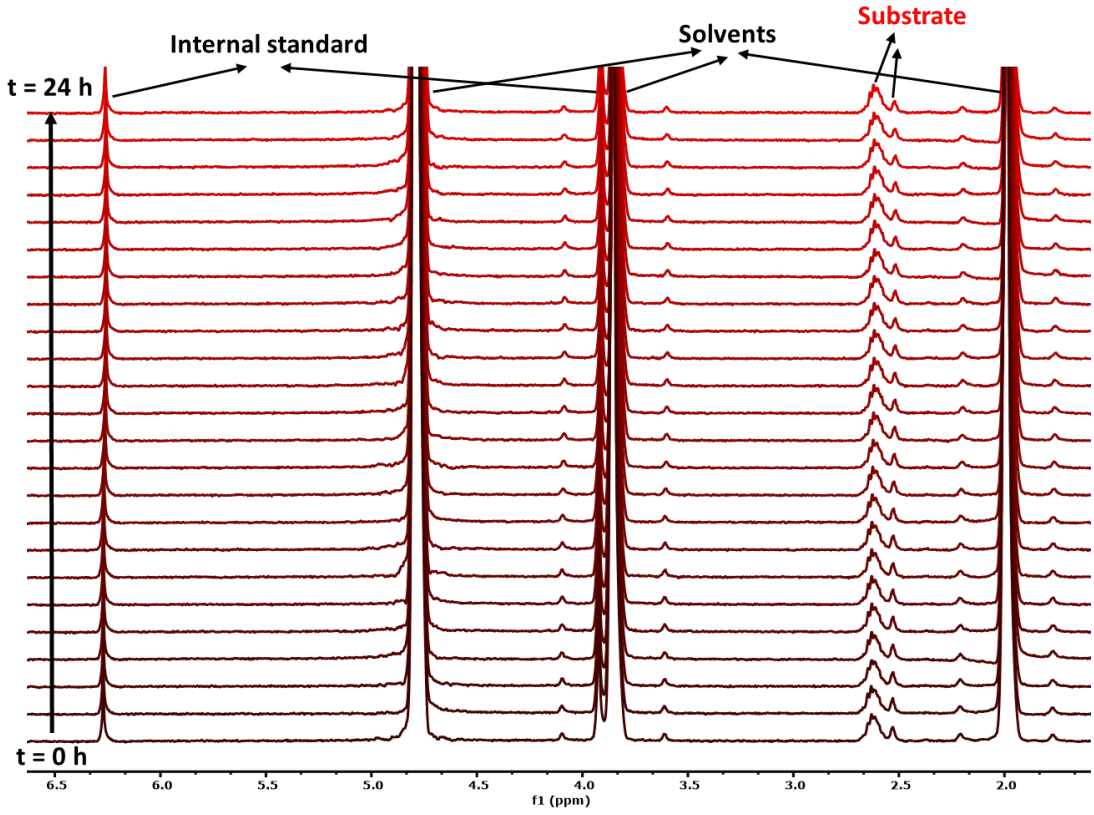

Figure S19. ^{1}H NMR (300 MHz, 298 K) monitored the catalytic reaction process every 1 h within 24 h after 365 nm UV light irradiating substrate 3 in THF-d_8:D_2O = 1:1 solution for 10 min. All the signals for the substrate 3, internal standard and solvents can be clearly assigned.

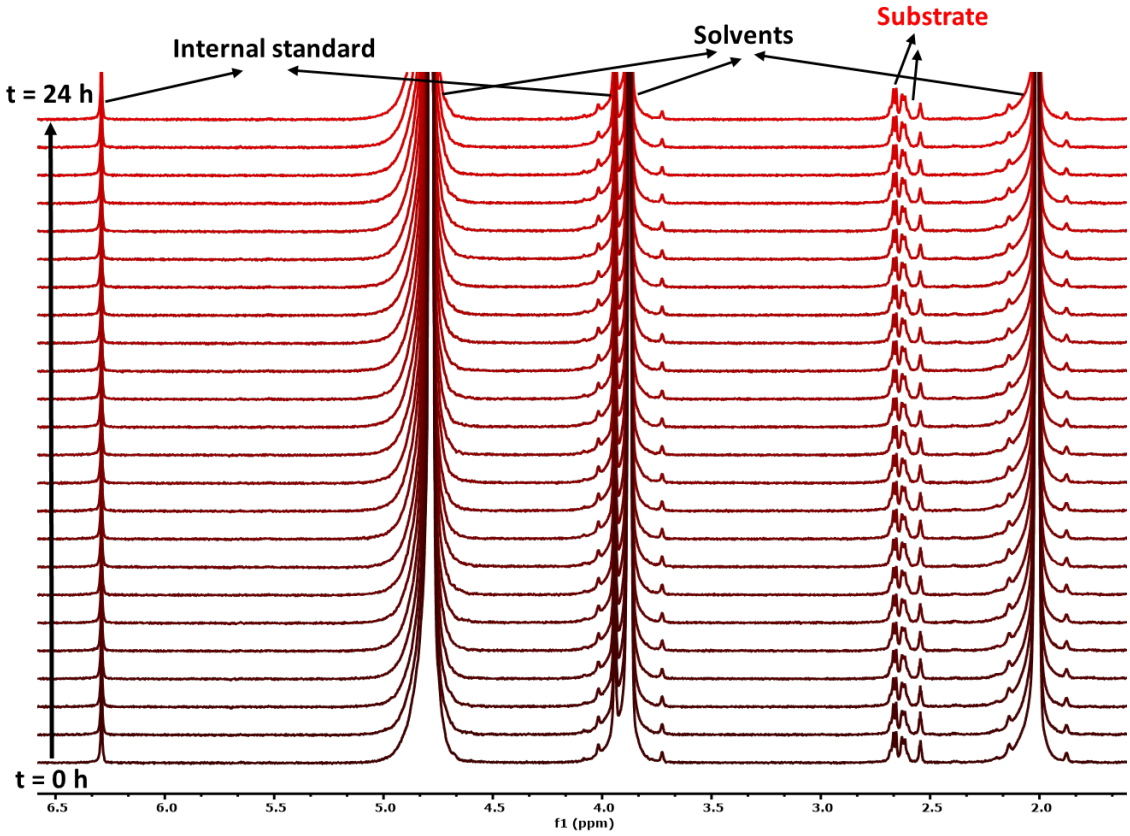

Figure S20. ^{1}H NMR (500 MHz, 298 K) monitored the catalytic reaction process every 1 h within 24 h after 470 nm blue light irradiating substrate 3 in THF-d_8:D_2O = 1:1 solution for 5 min. All the signals for the substrate 3, internal standard and solvents can be clearly assigned.

7. Computational study (DFT) for *trans*-Cat, *cis*-Cat structure optimization

The structures of complexes *trans*-Cat and *cis*-Cat were pre-optimized with GFN2-xTB,[6] and subsequently a conformational search was performed using the crest[7] procedure included within the xTB program package developed by Grimme and coworker.[8] We used an implicit solvation model for water in these procedures (alpb H_2O). The lowest energy structures from these crest conformational searches were selected for subsequent re-optimization at the DFT level.

All DFT calculations were performed using the Turbomole program package[9] coupled to the PQS Baker optimizer[10] via the BOpt package.[11] We used unrestricted ri-DFT-D3 calculations at the BP86 level,[12] in combination with the def2-SVP basis set[13] and a small (m4) grid size. Grimme's dispersion corrections[14] (version 3, disp3, 'zero damping') were used to include Vander Waals interactions. Optimized configurations are supplied in .pdb and .xyz format.

8. Steric maps and buried volume of *trans*-Cat and *cis*-Cat

The topographic steric map and %buried volume ($\%V_{Bur}$) of the optimized structure DFT (*trans*-Cat) and DFT (*cis*-Cat) were calculated by SambVca to show the steric hindrance of ligands. As shown in Figure S19, the west-side values (the total value of northwest and southwest), which represent the side of imidazolium ring without azobenzene, are similar (47.8% and 48.4% respectively). However, comparing the $\%V_{Bur}$ of east side (the total value of northeast and southeast), DFT (*cis*-Cat) (122.6%) is higher than the $\%V_{Bur}$ of DFT (*trans*-Cat) (117.3%), which results from the photoisomerization of azobenzene. This also suggested that *trans*-Cat showed a more beneficially spatial structure to coordinate substrate than *cis*-Cat, as the reason for reaction rate acceleration simultaneously.

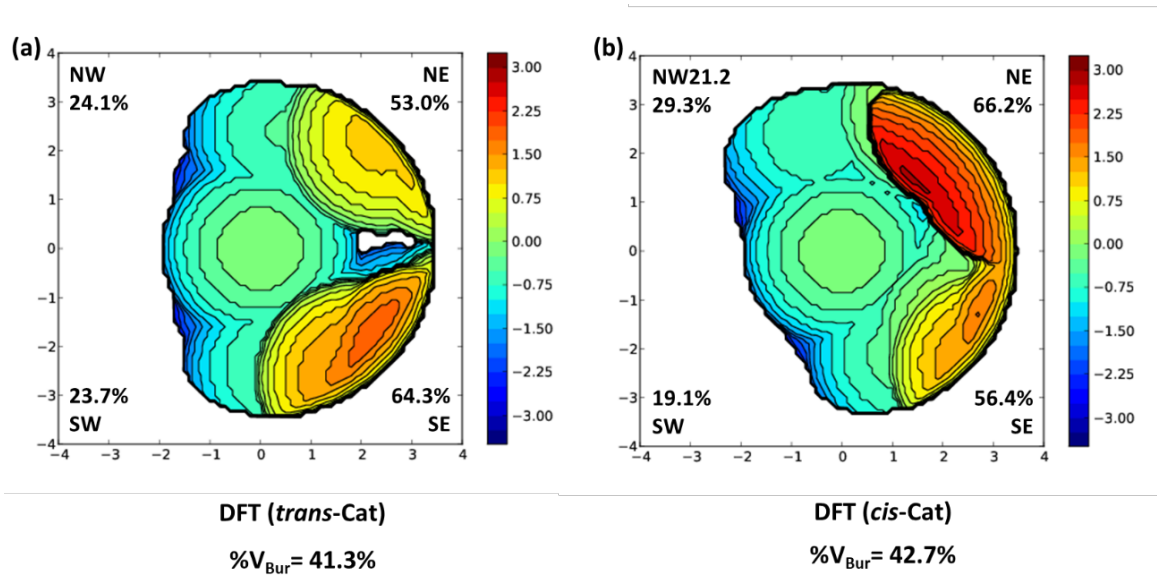

Figure S21. Topographic steric maps and buried volumes of (a) DFT (*trans*-Cat) and (b) DFT (*cis*-Cat) with quadrantal $\%V_{Bur}$ values.

9. References

1 X. Liao, G. Chen, X. Liu, W. Chen, F. Chen and M. Jiang, *Angew. Chem. Int. Ed.*, 2010, **49**, 4409-4413.

2 A. Wu, F. Lu, P. Sun, X. Gao, L. Shi and L. Zheng, *Langmuir*, 2016, **32**, 8163-8170.

3 M. Wegener, M. J. Hansen, A. J. M. Driessen, W. Szymanski and B. L. Feringa, *J. Am. Chem. Soc.*, 2017, **139**, 17979-17986.

4 G. Yu, C. Han, Z. Zhang, J. Chen, X. Yan, B. Zheng, S. Liu and F. Huang, *J. Am. Chem. Soc.* 2012, **134**, 20, 8711–8717.

5 M. R. Cunha, R. Bhardwaj, S. Lindinger, C. Butorac, C. Romanin, M. A. Hediger and J. L. Reymond, *ACS Med. Chem. Lett.*, 2019, **10**, 1341-1345.

6 C. Bannwarth, S. Ehlert and S. Grimme., *J. Chem. Theory Comput.*, 2019, **15**, 1652-1671.

7 (a) P. Pracht, F. Bohle, S. Grimme, *Phys. Chem. Chem. Phys.,* 2020, **22**, 7169-7192. (b) S. Grimme, *J. Chem. Theory Comput.* 2019, **15**, 5, 2847-2862.
8 C. Bannwarth, E. Caldeweyher, S. Ehlert, A. Hansen, P. Pracht, J. Seibert, S. Spicher, S. Grimme, *WIREs Comput. Mol. Sci.,* 2021, **11**:e1493.
9 TURBOMOLE Version 7.5.1 (TURBOMOLE Gmbh, Karlsruhe, Germany).
10 (a) PQS version 2.4, 2001, Parallel Quantum Solutions, Fayetteville, Arkansas, USA (the Baker optimizer is available separately from PQS upon request); (b) J. Baker, *J. Comput. Chem*. **1986**, *7*, 385-395.
11 P. H. M. Budzelaar, *J. Comput. Chem.* **2007**, *28*, 2226-2236.
12 (a) A. D. Becke, *Phys. Rev. A* **1988**, *38*, 3098-3100. (b) J. P. Perdew, *Phys. Rev. B* **1986**, *33*, 8822-8824.
13 (a) F. Weigend, R. Ahlrichs, *Phys. Chem. Chem. Phys.* **2005**, *7*, 3297-3305. (b) F. Weigend, M. Häser, H. Patzelt, R. Ahlrichs, *Chem. Phys. Lett.* **1998**, *294*, 143-152.
14 S. Grimme, J. Antony, S. Ehrlich, H. Krieg, *J. Chem. Phys.* **2010**, *132*, 154104.

10. Cartesian coordinates of optimized configurations of *trans*-Cat and *cis*-Cat

Trans-Cat

C	3.5487592	0.7480922	0.9039770
N	3.5008159	0.9137080	2.2639885
C	3.5876496	2.2591735	2.6039897
C	3.6902997	2.9572157	1.4281618
N	3.6621702	2.0188706	0.4013927
H	3.5848717	2.6017163	3.6430168
H	3.7880222	4.0300696	1.2393935
Au	3.4016699	-0.9656291	-0.1238612
Br	3.1580492	-3.0421489	-1.3660933
C	3.2759729	2.3316692	-0.9908165
H	3.7984649	1.6237353	-1.6613127
H	3.6263478	3.3586868	-1.2146610
C	3.0134519	-0.1519534	3.1624446
H	3.0517432	0.2492650	4.1950615

H	3.7040630	-1.0149255	3.0985968
C	1.7640657	2.1990518	-1.0983072
C	-1.0234758	1.7771707	-0.9171021
C	0.9392855	3.1219448	-0.4145417
C	1.1701973	1.0844918	-1.7243999
C	-0.2145681	0.8814510	-1.6477590
C	-0.4361845	2.9169642	-0.3130666
H	1.3899072	4.0069182	0.0630958
H	1.7974042	0.3506936	-2.2530861
H	-0.6875428	0.0089867	-2.1204342
H	-1.0887615	3.6203570	0.2225150
C	1.6062168	-0.5518813	2.7438280
C	-0.8819408	-1.1771867	1.5765992
C	1.3544389	-1.8517738	2.2636027
C	0.5925671	0.4294813	2.6458002
C	-0.6483026	0.1264254	2.0801415
C	0.1283621	-2.1574902	1.6622729
H	2.1465310	-2.6147926	2.2975699
H	0.7987729	1.4613423	2.9737155
H	-1.4367890	0.8852366	1.9667859
H	-0.0598842	-3.1482588	1.2254745
N	-2.0716465	-1.5658040	0.9254266
N	-2.4101488	1.5166805	-0.8772693
N	-3.1115168	-0.9260391	1.2658795

N	-3.0246831	2.0950535	0.0714637
C	-4.2736932	-1.2733422	0.5385254
C	-6.6745056	-1.9026197	-0.7742200
C	-4.2416685	-1.7895547	-0.7783929
C	-5.5095453	-1.0496652	1.1816848
C	-6.7048583	-1.3811969	0.5315630
C	-5.4422620	-2.0944309	-1.4294962
H	-3.2645974	-1.9273913	-1.2617867
H	-5.5006432	-0.6148780	2.1912984
H	-7.6674640	-1.2123637	1.0368283
H	-5.4227516	-2.4839302	-2.4592023
H	-7.6154626	-2.1448342	-1.2916831
C	-4.4304269	1.9864531	0.0439088
C	-7.2367451	1.9380562	0.1404953
C	-5.1073539	2.4220923	1.2044212
C	-5.1670998	1.5254885	-1.0747828
C	-6.5624990	1.5071001	-1.0204303
C	-6.5075002	2.3893151	1.2542300
H	-4.5044184	2.7764358	2.0532585
H	-4.6146212	1.1896600	-1.9627955
H	-7.1377151	1.1440694	-1.8853289
H	-7.0340097	2.7228253	2.1613351
H	-8.3368145	1.9191429	0.1740869

C*is*-Cat

C	-1.6800241	1.9437624	-0.7683764
N	-1.5766945	2.0508111	-2.1327250
C	-0.9448174	3.2348128	-2.4924258
C	-0.6504912	3.8940126	-1.3268523
N	-1.1103399	3.0924190	-0.2874800
H	-0.7685343	3.5101932	-3.5364447
H	-0.1499201	4.8499565	-1.1488976
Au	-2.3508569	0.3359352	0.2315304
Br	-3.0945077	-1.6803996	1.3751622
C	-0.6885413	3.2653578	1.1147047
H	-1.3978038	2.6834363	1.7351033
H	-0.7862215	4.3361103	1.3797527
C	-1.7818203	0.8991863	-3.0210232
H	-1.6255434	1.2548398	-4.0608030
H	-2.8353683	0.5656864	-2.9359328
C	0.7393691	2.7746705	1.2791190
C	3.4045624	1.8351790	1.3452218
C	1.0188574	1.3942654	1.1797625
C	1.8119841	3.6747153	1.4452228
C	3.1334837	3.2105067	1.5126811
C	2.3324077	0.9251160	1.1961124
H	0.1961511	0.6698753	1.0670218
H	1.6113148	4.7542968	1.5399033
H	3.9726484	3.9023041	1.6773856

H	2.5352940	-0.1507373	1.1232737
C	-0.8401962	-0.2398581	-2.6534328
C	0.8068679	-2.3587564	-1.7659985
C	-1.2420776	-1.5790545	-2.8242529
C	0.4165053	0.0214220	-2.0657227
C	1.2219229	-1.0186165	-1.6020273
C	-0.4122240	-2.6326260	-2.4219086
H	-2.2289678	-1.8038405	-3.2578465
H	0.7612903	1.0555459	-1.9115580
H	2.1742370	-0.8001923	-1.1052673
H	-0.7179185	-3.6794488	-2.5625182
N	1.6621114	-3.4482067	-1.4408367
N	4.7438495	1.3825820	1.5217212
N	2.2389120	-3.5973735	-0.3336713
N	5.2957369	0.5304050	0.7827727
C	1.9383330	-2.8507209	0.8471655
C	1.5507695	-1.6387204	3.3625012
C	3.0157219	-2.7230057	1.7564988
C	0.6471325	-2.4055178	1.2294315
C	0.4625697	-1.8175709	2.4876560
C	2.8307003	-2.0920999	2.9935194
H	3.9909706	-3.1369599	1.4638588
H	-0.2254852	-2.5328749	0.5729022
H	-0.5533686	-1.4979753	2.7673381

H	3.6834480	-1.9679480	3.6776140
H	1.3967652	-1.1572355	4.3397850
C	4.7832867	0.1123554	-0.4833644
C	4.1431913	-0.7976875	-3.0723032
C	4.9539457	-1.2484628	-0.8242573
C	4.3117990	1.0247821	-1.4597667
C	4.0160022	0.5666121	-2.7506712
C	4.6015418	-1.7059991	-2.1008799
H	5.3625740	-1.9310904	-0.0665871
H	4.2065709	2.0889855	-1.2051539
H	3.6667713	1.2802770	-3.5125565
H	4.6866854	-2.7762671	-2.3381807
H	3.8804379	-1.1541697	-4.0789990